

Deep Speech Synthesis from Articulatory Features

Anonymous ACL submission

Abstract

In the articulatory synthesis task, speech is synthesized from input features containing information about the physical behavior of the human vocal tract. This task provides a promising direction for speech synthesis research, as the articulatory space is compact, smooth, and interpretable. Current works have highlighted the potential for deep learning models to perform articulatory synthesis. However, it remains unclear whether these models can achieve the efficiency and fidelity of the human speech production system. To help bridge this gap, we propose a time-domain articulatory synthesis methodology and demonstrate its efficacy with both electromagnetic articulography (EMA) and synthetic articulatory feature inputs. Our model is both computationally efficient and highly intelligible, achieving a transcription word error rate (WER) of 7.14% for the EMA-to-speech task. Through interpolation experiments, we also highlight the generalizability and interpretability of our approach.

1 Introduction

Speech synthesis has seen rapid development in recent years with deep learning based techniques. These models have shown success in tasks like text-to-speech (TTS) (Wang et al., 2017; Hayashi et al., 2021; Prenger et al., 2019), speech-to-speech translation (S2ST) (Tjandra et al., 2019; Jia et al., 2019; Inaguma et al., 2020), voice conversion (VC) (Polyak et al., 2021; Wu et al., 2021a; Sisman et al., 2020), and more (Anumanchipalli et al., 2019; Yu et al., 2019; Gaddy and Klein, 2021). Moreover, this technology has yielded impactful technologies like speech synthesis aids for people with blindness or paralysis (Karmel et al., 2019; Angrick et al., 2019; Anumanchipalli et al., 2019). While speech synthesizers have already shown promising results for assistive tasks in healthcare and other challenging domains, technologies like brain-to-speech devices are still nascent and require new

algorithms in order to be deployed as high-fidelity, open-vocabulary synthesizers. To this end, our work focuses on devising a deep speech synthesis methodology that is computationally efficient, real-time, and high-fidelity. We propose a time-domain articulatory synthesis approach that is suitable for attaining these three properties and empirically validate our method on two distinct articulatory modalities, EMA and a synthetic articulatory space. Our deep learning models also exhibit valuable interpretability properties, which we demonstrate through interpolation experiments.

We proceed by discussing speech synthesis in the context of deep learning and articulatory synthesis in Section 2. In Section 3, we describe our deep articulatory models and time-domain methodology. Then, we discuss the two articulatory datasets chosen for our empirical studies and their respective modalities in Section 4. With these datasets, we conduct computational efficiency, interpolation, and synthesis quality studies, discussed in Sections 5, 6, and 7, respectively. We then provide further analyses with respect to phoneme confusability in Section 8. Finally, we summarize our results and propose future directions in Section 9. Audio samples and additional related information are all available at <https://articulatorysynthesis.github.io>.

2 Speech Synthesis

2.1 Deep Speech Synthesis

Currently, state-of-the-art speech synthesis algorithms use deep learning (Hayashi et al., 2021; Anumanchipalli et al., 2019; Jia et al., 2021; Polyak et al., 2021; Gaddy and Klein, 2021). While existing methods can generate high-fidelity speech, they tend to be computationally expensive and difficult to interpret and generalize (Nekvinda and Dušek, 2020; Zhang et al., 2019). We attribute underspecification to the primary cause of these issues, as speech data is very high dimensional

and current algorithms lack sufficient inductive biases. To help bridge this gap, we devise deep articulatory synthesis techniques that exhibit suitable computational efficiency, generalizability, and interpretability properties by behaving more similarly to the human speech production process than existing methods.

2.2 Articulatory Synthesis

Articulatory synthesis generally refers to the task of synthesizing speech from articulatory features, i.e., features containing information about the physical behavior of the human vocal tract (Fant, 1991; Rubin et al., 1981; Scully, 1990). We identify two primary research directions in articulatory synthesis: 1. modelling the human vocal tract (Fant, 1995; Iskarous et al., 2003; Birkholz, 2013a), and 2. learning the mapping from articulatory features to speech through a statistical means (Aryal and Gutierrez-Osuna, 2016; Bocquelet et al., 2014; Chen et al., 2021). The former direction, due to its focus on computational modelling, has yielded articulatory synthesizers that are interpretable and relatively space-efficient but computationally slow. On the other hand, the latter direction has yielded methods that are much faster but have worse interpretability and memory efficiency. Ideally, speech synthesizers should have low space and time complexities, which would enable many impactful real-time applications. For example, such systems could allow patients with paralysis or aphasia to communicate naturally at any moment in time. Thus, we focus on making methods in the second research direction more memory-efficient in this work. Additionally, we highlight how statistical articulatory synthesis methods could also be highly interpretable, thus containing all of the benefits of articulatory synthesizers built using physical modelling.

We also focus on the statistical research direction in this work because of the transferability of our methodology to all forms of speech synthesis. Current state-of-the-art speech synthesis systems rely on an intermediate speech representation, typically a spectrum or a learned representation (Kong et al., 2020; Morrison et al., 2022; Badlani et al., 2021; Kim et al., 2021; Elias et al., 2021). Inductive biases offer one potential way of making these models efficient, generalizable, and interpretable as mentioned in Section 2.1. Constraining these intermediate representations to an articulatory feature

space is one way to impose such an inductive bias, especially since there is a limited set of articulator configurations that can completely specify all possible human speech. The resulting model would then need to perform an articulatory-to-speech mapping, of which the behavior is relatively unknown to our knowledge. This work aims to bridge this gap by studying the efficiency, generalizability, interpretability, and fidelity of such a mapping using two distinct articulatory modalities, EMA and a synthetic one generated using a vocal tract model, detailed in Section 4.

While deep EMA-to-speech models have been previously studied, as far as we are aware (Taguchi and Kaburagi, 2018; Stone et al., 2020; Liu et al., 2018), current models are not highly intelligible, achieving a transcription WER of around 30% on open-vocabulary tasks (Taguchi and Kaburagi, 2018). In this work, we build an EMA-to-speech model that achieves a transcription WER of 7.14% and perform detailed error analyses on the synthesized utterances. We also extend this approach to building a speech synthesizer using a synthetic articulatory modality. This model is efficient, high-fidelity, and interpretable, which has previously been unattained to our knowledge. We detail these models and our proposed time-domain articulatory synthesis methodology in Section 3 below.

3 Deep Articulatory Models

3.1 Frequency- and Time-Domain Modeling

Similarly to the state-of-the-art speech synthesis works discussed in Section 2, current deep articulatory synthesis works rely on synthesizing an intermediate spectrum representation, from which waveforms are generated (Csap'o et al., 2020; Georges et al., 2020). Since this behavior is not present in the human speech production process, we propose a model that directly maps articulatory features to waveforms in this work. Since this model does not explicitly rely on a frequency-based intermediate, we refer to this approach as a time-domain one. This modification noticeably improves model efficiency while achieving comparable intelligibility on our two datasets, as discussed in Sections 5 and 7. We proceed to discuss our spectrum-intermediate baseline in Section 3.2 and our two time-domain methods in Sections 3.3 and 3.4.

178 3.2 Spectrum-Intermediate Baseline

179 For our baseline deep learning model, we build
180 on the state-of-the-art articulatory synthesis archi-
181 tecture proposed by Gaddy and Klein (Gaddy and
182 Klein, 2021). Namely, we map articulatory fea-
183 tures to spectrums using a six-layer Transformer
184 (Vaswani et al., 2017) prepended with three resi-
185 dual convolution blocks. To map spectrums to
186 waveforms, we use HiFi-GAN (Kong et al., 2020),
187 which has been shown to perform better than the
188 WaveNet vocoder used by Gaddy and Klein (Gaddy
189 and Klein, 2021). For our spectrum representation,
190 we use Mel spectrograms instead of MFCCs, as
191 done in the HiFi-GAN paper and most deep speech
192 synthesis works (Kong et al., 2020; Wang et al.,
193 2017; Hayashi et al., 2021).

194 We also modify the loss function used by Gaddy
195 and Klein (Gaddy and Klein, 2021). To avoid re-
196quiring phoneme annotations to train the model, we
197 omit the phonemic loss. We instead improve model
198 performance by adding the adversarial loss used
199 by HiFi-GAN (Kong et al., 2020). Since our data
200 in this work has sequences of articulatory features
201 that are pre-aligned with waveforms, we also do not
202 need the dynamic time warping loss. We refer to
203 this resulting baseline as the spectrum-intermediate
204 (Spec.-Int.) model below.

205 In all of our experiments, we train the Trans-
206 former model using the Adam optimizer (Kingma
207 and Ba, 2015) with a learning rate of $3.0 * 10^{-5}$ for
208 both the generator and the discriminators, a batch
209 size of 32, and loss balancing coefficients match-
210 ing those used with the original HiFi-GAN model
211 (Kong et al., 2020). Our discriminator architec-
212 tures and HiFi-GAN spectrum-to-speech vocoder
213 parameters also match those of Kong et al. (Kong
214 et al., 2020), and our Transformer has a hidden
215 dimension of 1024 and a dropout rate of 0.2.

216 3.3 Time-Domain HiFi-GAN

217 For our first time-domain model, we feed our ar-
218 ticulatory input features directly into HiFi-GAN
219 (Kong et al., 2020), keeping the architecture and
220 loss functions the same while changing the input
221 modality. To our knowledge, directly feeding ar-
222 ticulatory inputs into a deep vocoder architecture
223 has not yielded any successful results previously.
224 However, we observe that this model is compara-
225 ble to our baseline, as discussed in Section 7.
226 Moreover, removing the need for an articulatory-
227 to-spectrum architecture noticeably improves com-

putational efficiency, as discussed in Section 5. For
228 all of our experiments, we optimize this model us-
229 ing the same hyperparameters as the HiFi-GAN
230 spectrum-to-speech vocoder used in the Section
231 3.2 baseline above.

232 3.4 NSF-CAR Model

233 For our second time-domain model, we build on the
234 neural source-filter (NSF) architecture (Wang et al.,
235 2019). Since articulatory features can be divided
236 into source- and filter-related attributes (Birkholz,
237 2013a), we experiment with this architecture in
238 order to study whether explicitly modelling this
239 separation could improve articulatory synthesis per-
240 formance.

241 Similarly to our baseline, we use the loss func-
242 tion from HiFi-GAN to improve synthesis fidelity.
243 We also leverage autoregression to improve the
244 pitch and periodicity of model outputs and make
245 our model a streaming-based one. Namely, we
246 incorporate the autoregressive encoder from CAR-
247 GAN (Morrison et al., 2022) into our model, con-
248 catenating its output with each vector in the condi-
249 tion module input sequence. We replace the convo-
250 lutions in the NSF condition module with GBlock
251 layers (Morrison et al., 2022), which we found to
252 further improve model performance. Figure 7 in
253 the Appendix depicts the architecture of our gener-
254 ator.

255 To our knowledge, neural source filter mod-
256 els are currently only used for building vocoders
257 that map spectrums to speech (Wang et al., 2019;
258 Georges et al., 2020). In this work, we leverage
259 source-filter modelling to perform articulatory syn-
260 thesis without relying on an intermediate spectrum
261 representation.

262 3.5 WSOLA

263 As observed by Morrison et al. (Morrison et al.,
264 2022), simply concatenating the output chunks gen-
265 erated through an autoregressive process yields arti-
266 facts at the concatenation points. Thus, during eval-
267 uation, we join outputs using an approach based
268 on WSOLA. Namely, we overlap-and-add adjacent
269 output chunks at intersections with maximum cross-
270 correlation, sliding the chunks up to a distance of
271 one pitch period. We calculate a pitch period by
272 multiplying the sampling rate with the reciprocal
273 of the last F0 value in the first chunk input. Figure
274 1 depicts one such WSOLA operation.

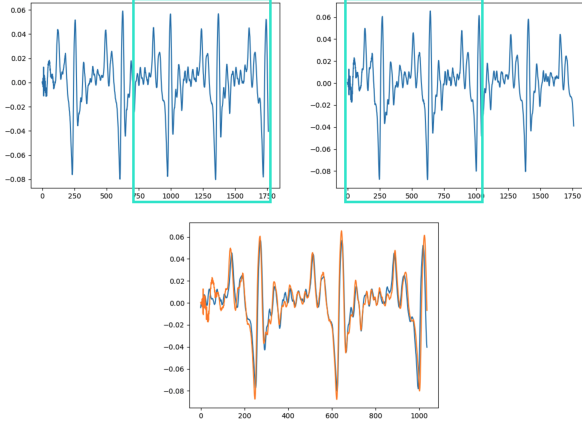


Figure 1: WSOLA-based method for concatenating waveforms.

4 Datasets

4.1 Electromagnetic Articulography (EMA)

For our first task, we perform EMA-to-speech using the MNGU0 dataset (Richmond et al., 2011), which contains 67 minutes of single-speaker speech recorded at 16 kHz annotated with 12-dimensional EMA features recorded at 200 Hz. We use the train-test split provided in the original work, which has 1,129 utterances for training and 60 for testing. Among the 1,129 training utterances, we set off a random size-60 subset for validation. Since EMA on its own does not contain voicing information, we concatenate estimated F0 sequences extracted using CREPE (Kim et al., 2018; Morrison et al., 2022) to the EMA features, forming a 13-dimensional input feature.

4.2 Synthetic Articulatory Features

Since EMA data does not contain enough manner information to perfectly reconstruct the original speech, we also experiment with synthetic articulatory data that does. Namely, we use the vocal tract model from Birkholz et al. (Birkholz, 2013a) to create a single-speaker corpus of pseudo-words, each composed of two to three vowel and consonant sounds. Our training set has 10,000 such utterances, and our validation set has 250, totaling a few hours of speech. For our evaluation set, we use the Birkholz vocal tract model outputs corresponding to the first 99 phoneme sequences in the CMU US KAL Diphone database (Lenzo and Black, 2000). All waveforms have a sampling rate of 44100 Hz and articulatory features are recorded every 110 samples. We refer to this dataset as the Birkholz-Pseudoword (Birk.-Pseudo.) dataset be-

low. In this dataset, our articulatory features are 30-dimensional.

5 Computational Efficiency

Computational efficiency during training is essential for low-resource speech synthesis tasks like brain-to-speech and other articulatory synthesis tasks where data collection is expensive. During inference, computational efficiency is essential for building real-time speech synthesizers, e.g., for brain-to-speech. We observe that our time-domain articulatory synthesis model has some suitable computational efficiency properties compared to the frequency-domain baseline. As shown in Table 1, our model is able to train twice as fast as the baseline on a single RTX 2080 Ti GPU for the task with synthetic articulatory data. While our model synthesizes utterances slower than the baseline due to the nature of autoregression (Morrison et al., 2022), we observe that generation on a CPU is still faster than real-time.

Compared to the baseline, our time-domain models are much more memory efficient, as detailed in Table 2. Our models are able to use over 8 to 20 times less number of parameters than the baseline due to their ability to directly map articulatory features to speech. Namely, while current articulatory synthesis models like our baseline rely on two components, one to output spectrums and another to convert spectrums to waveforms, our time-domain models only contain one. We note that the real-time and memory efficient properties of our time-domain models make them a viable choice for streaming, on-device tasks.

Data	Birk.-Pseudo.	EMA-MGNU0
NSF-CAR	34	81
HiFi-GAN	8	9
Spec.-Int.	68	80

Table 1: Total training time for each model in hours.

Model	Birk.-Pseudo.	EMA-MGNU0
NSF-CAR	$4.4 * 10^6$	$4.2 * 10^6$
HiFi-GAN	$14.2 * 10^6$	$12.6 * 10^6$
Spec.-Int.	$98.7 * 10^6$	$94.0 * 10^6$

Table 2: Number of parameters of each model.

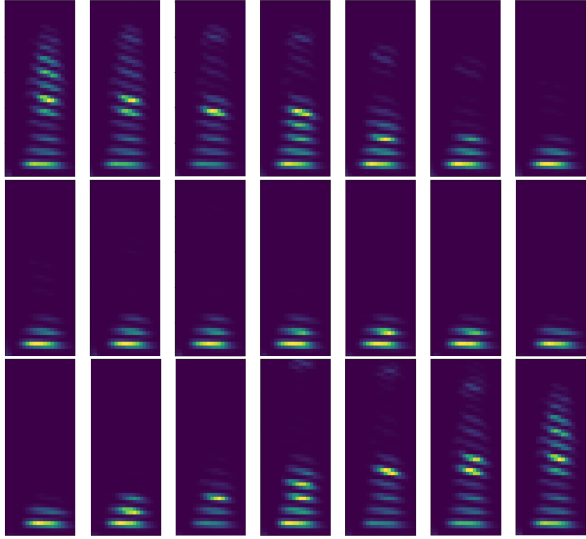


Figure 2: Vowel interpolation. The top row contains the synthesized samples between the "ta" and "tu" sounds, the middle row "tu" and "ti", and the bottom row "ti" and "ta".

6 Interpolation

6.1 Vowel Interpolation

To study the generalizability of our time-domain model, we perform interpolation experiments. First, to analyze how well our model generalizes across vowel sounds, we perform vowel interpolation. Namely, we interpolate between the "ta" and "tu" sounds, "tu" and "ti", and "ti" and "ta" using the synthetic articulatory data. We generate the articulatory features for "ta", "tu", and "ti" using the code provided by Birkholz et al., similarly to our approach for creating the synthetic articulatory dataset described above. For each of the three pairs of sounds, we perform a linear interpolation between the two articulatory features, generating seven evenly spaced weighted combinations. The figures below are generated using outputs from our NSF-CAR model, and we observe similar trends with our time-domain HiFi-GAN as well, which we include in the supplementary website linked in Section 1.

Figure 2 contains the mel-spectrograms of the generated speech from our model for each of these combined articulatory features. Our model is able to generalize to the unseen articulatory features between the three sounds. Moreover, the transitions between spectrum values in each interpolation are smooth, suggesting that our network is able to model the continuity of articulator movements, at least with respect to vowels.

6.2 Consonant Interpolation

We also study the generalizability of our model with respect to consonants. To study how well our model generalizes across types of consonant sounds, we fix the place of articulation and interpolate between consonant types. Namely, we interpolate between the alveolar consonants "ra", "na", and "la", using the same methodology as our vowel interpolation experiment in Section 6.1.

Figure 3 depicts the mel-spectrograms of synthesized interpolation samples from our time-domain articulatory synthesis model. Similarly to our vowel interpolation results, we observe that our model generalizes to the unseen samples between the three consonants and exhibits smooth generation. Specifically, these results indicate that our model can smoothly transition between nasal, approximant, and lateral approximant consonants, similarly to the human speech production process.

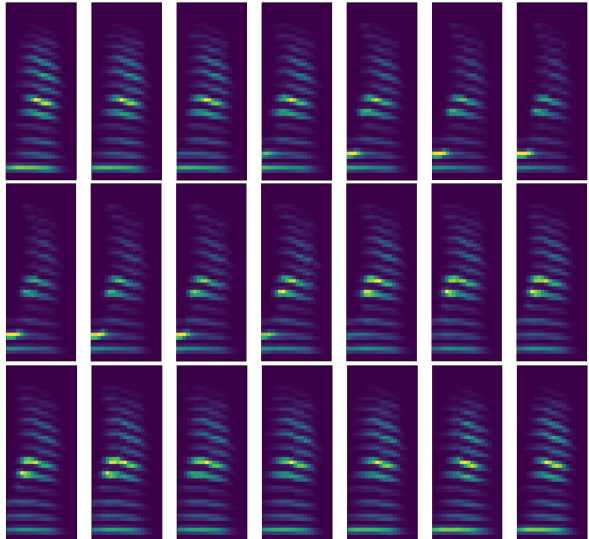


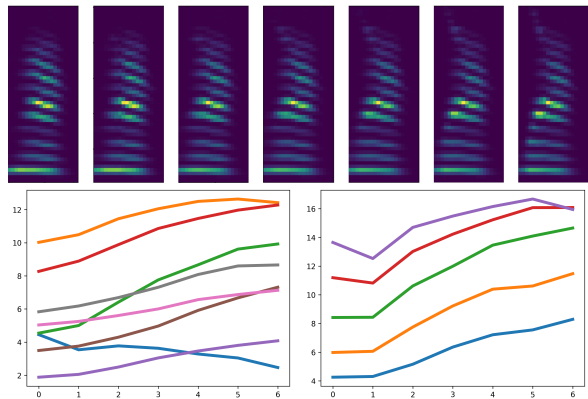
Figure 3: Alveolar consonant interpolation. The top row contains the synthesized samples between the "ra" and "na" sounds, the middle row "na" and "la", and the bottom row "la" and "ra".

To study how well our model generalizes across place of articulation, we fix the consonant type and interpolate between two places. Namely, we interpolate between the approximant consonants "ra" and "ja", using the same aforementioned methodology. Figure 4 depicts these results. As with our alveolar consonant interpolation results, we observe that our model generalizes to unseen samples and produces smooth transitions between synthesized interpolation samples here.

To quantify how the synthesized utterances

403
404
405
406
407
408
409
410
411
412
413
414
415
416
417
418
419
420
421
422
change across the interpolation, we create two plots
studying changes in the magnitudes of different
bands of the mel-spectrogram. Namely, our first
graph plots the magnitude of each mel-spectrogram
frequency vector across the seven utterances, going
left to right in the interpolation. Our second plot
does the same with time vectors, i.e., columns in
the mel-spectrograms. We compute the magnitude
of each vector using the L1 norm, which is just a
sum here since mel-spectrogram values are non-
negative. To improve readability in both plots, we
omit vectors that on average change less than 0.3 in
magnitude between adjacent interpolation samples.

As shown in the bottom row of Figure 4, the
vector magnitude lines are generally monotonic and
almost linear in many cases when going left to right
in the interpolation. This supports our hypothesis
that our model has learnt to transition smoothly
between consonants when synthesizing articulatory
features.



423
424
425
426
427
428
429
430
431
432
433
434
435
Figure 4: Approximate consonant interpolation. *Top row*: synthesized samples between the "ra" and "ja"
sounds. *Bottom row left*: frequency vector magnitudes for each spectrum. *Bottom row right*: time vector
magnitudes for each spectrum.

6.3 Interpretability

We note that these interpolation results also highlight the interpretability of articulatory features. Namely, we are able to simply take an element-wise weighted sum of two same-length sequences of articulatory features in order to create the utterance corresponding to articulator movements in between the two gestures. For example, to create the "te" sound, we would just need to synthesize the average of the articulatory feature sequences for "ti" and "ta". To our knowledge, this degree of interpretability is not supported by other speech representations like spectrums or deep-learning-based

436
ones.

7 Synthesis Quality

7.1 Fidelity

439
440
441
442
443
444
445
446
447
448
449
450
451
452
453
454
Since MCD serves as an objective measure of synthesis quality (Black, 2019), we first measure synthesis fidelity using this metric. As detailed in Table 3, we observe that our time-domain articulatory synthesis approach achieves performance comparable to the frequency-domain baseline. Namely, our approach performs noticeably better than the baseline on the synthetic articulatory dataset and slightly worse on the EMA-to-speech task. Given these results, we attribute the performance drop of our model on the EMA task to information loss within in the input data. Namely, the model appears to confuse phonemes due to the lack of manner information in the EMA inputs, which can be heard in the accompanying samples. We discuss this phoneme confusion in more detail below.

Model	MCD	
	Birk.-Pseudo	EMA-MGNU0
NSF-CAR	3.36 ± 0.28	5.44 ± 0.67
HiFi-GAN	2.90 ± 0.22	4.81 ± 0.76
Spec.-Int.	5.15 ± 0.48	4.75 ± 0.81

455
456
457
458
459
460
461
462
463
464
465
466
467
468
469
470
471
Table 3: MCD for each model on Birkholz and EMA data.

7.2 Automatic Speech Recognition

456
457
458
459
460
461
462
463
464
465
466
467
468
469
470
471
To evaluate the intelligibility of our synthesis approach, we conduct open-vocabulary transcription experiments for the EMA-to-speech task with our time-domain HiFi-GAN model described in Section 3.3. First, we perform an objective evaluation using deep automatic speech recognition (ASR) models. Specifically, we use DeepSpeech¹ (Hannun et al., 2014) as done by Gaddy and Klein (Gaddy and Klein, 2021) as well as the ESPnet Conformer ASR model trained on LibriSpeech² (Guo et al., 2021; Panayotov et al., 2015). We use these models to transcribe the synthesis outputs of our model on the entire MNGU0 evaluation set described in Section 4.1 and calculate the average word error rates (WERs) and character error rates (CERs). Since some utterances in the evaluation set contain proper nouns, we also compute ASR

¹<https://github.com/mozilla/DeepSpeech>

²<https://zenodo.org/record/4604066#.YeNA0i2z2CM>

473 metrics on all of the evaluation set utterances composed entirely of common nouns, which form a
474 32-utterance subset.
475

476 Table 4 summarizes our ASR results. On the
477 common-noun subset, our model achieves a character error rate of 10.7% with the ESPnet ASR model,
478 indicating that our model is able to synthesize intel-
479 ligible speech. The consistent differences between
480 the WER and CER values as well as the entire set
481 and common-noun subset performances suggests
482 that these ASR metrics may be underestimating
483 intelligibility, as also observed by Gaddy and Klein
484 ([Gaddy and Klein, 2021](#)). Thus, we also eval-
485 uate the intelligibility of our model though human
486 evaluations, as discussed in Section 7.3 below.
487

ASR Model	WER		CER	
	All	Com.	All	Com.
ESPnet	32.9	19.2	17.9	10.7
DeepSpeech	41.3	32.9	20.2	15.5

488 Table 4: ASR. entire evaluation set (All) and common
489 noun subset (Com.).
490

491 7.3 Human Evaluation

492 To further understand the intelligibility of our time-
493 domain articulatory synthesis approach, we also
494 perform open-vocabulary transcription tests with
495 human listeners, evaluating our same time-domain
496 HiFi-GAN model (Section 3.3) used in our Section
497 7.2 ASR experiments above. Namely, we randomly
498 select ten utterances from our EMA corpus evalua-
499 tion set, choosing among the 32 sentences without
500 proper nouns. Based on the transcriptions from
501 six English-speaking listeners, our model achieves
502 an average WER of 7.14%, indicating that our
503 model is able to produce intelligible speech. To
504 our knowledge, this value is noticeably lower than
505 prior results, which are around 30.1% ([Taguchi](#)
506 and [Kaburagi, 2018](#)). This suggests that our time-
507 domain articulatory synthesis methodology is a
508 suitable approach for efficiently performing speech
509 synthesis while achieving high intelligibility.

510 8 Phoneme Confusion

511 To further study the phonological errors made by
512 our model, we analyze the phonemes that our
513 EMA-to-speech model confused during synthe-
514 sis. Namely, we study phoneme confusability for
515 our time-domain HiFi-GAN model (Section 3.3)
516 through the transcriptions, both from the ASR ones
517 described in Section 7.2 and the human ones de-
518 scribed in Section 7.3. For each transcribed ut-
519 terance, we convert the graphemes to a phoneme
520 sequence using Phonemizer³ ([Bernard and Titeux,](#)
521 [2021](#)) and their eSpeak NG backend,⁴ and repeat
522 this grapheme-to-phoneme conversion with the
523 ground truth texts. We identify the phoneme con-
524 fusion pairs using sclite,⁵ which aligns each predicted
525 sequence with the respective ground truth and then
526 records the substitution errors.

527 For our human evaluation analysis, we use all
528 of the transcripts from the six listeners, i.e., 60 ut-
529 terances. Figure 5 depicts the resulting phoneme
530 confusion pairs. We plot these confusion pairs on
531 an International Phonetic Alphabet (IPA) chart that
532 extends the one from Gaddy and Klein to more
533 phonemes ([Gaddy and Klein, 2021](#)), indicating
534 pairs with a higher frequency of substitution errors
535 using darker lines. We also populate this IPA chart
536 with our confusion pairs from the ASR transcrip-
537 tions in Figure 6, for which we use the texts trans-
538cribed by the ESPnet model for the entire MNGU0
539 evaluation set, as discussed in Section 7.2. We omit
540 the phoneme pairs that are only confused once in
541 Figure 6 in order to improve readability.

542 From these two IPA charts, we observe that the
543 most of the word substitution errors are due to plo-
544 sive or vowel confusions. Since the primary vowel
545 confusions in Figure 5 differ from those in Figure 6,
546 we hypothesize that vowel confusability for human
547 evaluators mainly resulted from the substitution
548 of vowels to form logical, grammatically correct
549 words and phrases. The automatic transcribers may
550 not have as much of such bias and we observe
551 that the primary confused vowel pairs are relatively
552 close to each other with our ASR-based results,
553 reinforcing this hypothesis. One potential reason
554 for the plosive substitutions is that plosives gener-
555 ally have a shorter duration than other consonant
556 types like fricatives ([Alwan et al., 2011](#)) and thus
557 may be more readily confusable. Among the plo-
558 sives, "p", "b", "t", and "d" may have been easier to
559 confuse than "k" and "g" for the human evaluators
560 because the latter two plosives have longer voice
561 onset times, a pattern also observed by Birkholz
562 ([Birkholz, 2013b](#)). From Figure 6, we also observe
563 that multiple voiced-unvoiced pairs are confused.
564 We hypothesize that this is because the only voic-

³<https://github.com/bootphon/phonemizer>

⁴<https://github.com/espeak-ng/espeak-ng>

⁵<https://github.com/usnistgov/SCTK>

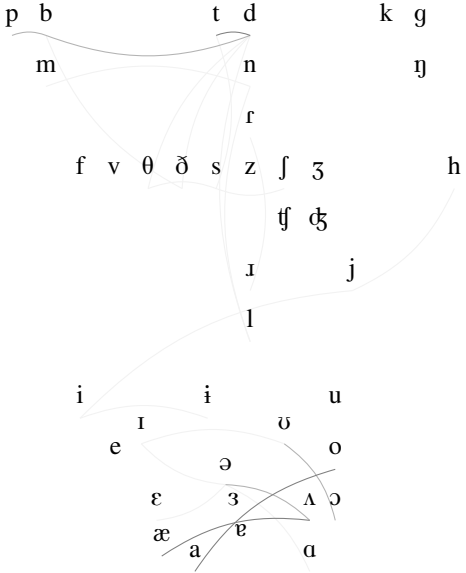


Figure 5: Phoneme confusability based on human transcriptions. Phoneme pairs that are confused more frequently have darker lines.

ing information that our EMA-to-speech model receives as input is the estimated F0 sequence, as described in Section 4.1.

9 Conclusion and Future Directions

In this work, we study ways to build deep articulatory synthesizers that are efficient and high-fidelity. Based on computational efficiency evaluations, we observe that our proposed time-domain methodology is suitable for achieving time and space complexities that are noticeably lower than the baseline spectrum-intermediate approach. Our interpolation study also highlights the generalizability and interpretability of our approach. Through MCD, ASR, and human transcription experiments, we demonstrate that our model is also highly intelligible, achieving a transcription word error rate (WER) of 7.14% for the EMA-to-speech task. Moving forward, we plan to test our methodology on other modalities like electromyography (EMG) (Gaddy and Klein, 2021) and real-time magnetic resonance imaging (RT-MRI) (Lim et al., 2021). We also plan to extend our approach to multi-speaker and multilingual settings (Richmond et al., 2011; Lim et al., 2021; Wu et al., 2021b).

References

- Abeer Alwan, Jintao Jiang, and Willa Chen. 2011. Perception of place of articulation for plosives and fricatives in noise. *Speech communication*, 53(2):195–209.

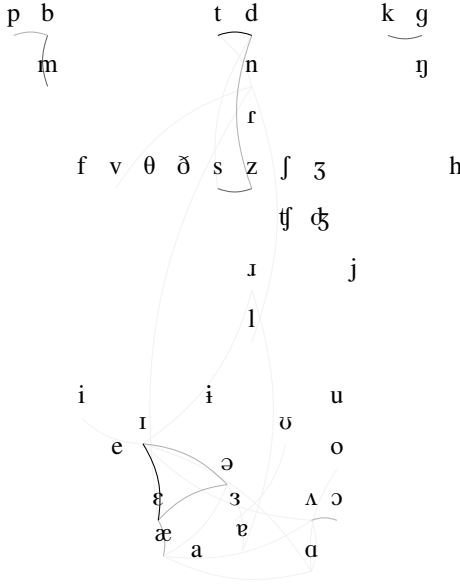


Figure 6: Phoneme confusability based on ASR transcriptions. Phoneme pairs that are confused more frequently have darker lines.

562
563
564

565
566
567
568
569
570
571
572
573
574
575
576
577
578
579
580
581
582
583
584
585

591
592
593
594
595

596
597
598

599
600
601
602

603
604
605
606

607
608
609
610

611
612
613

614
615
616

617
618

Miguel Angrick, Christian Herff, Emily Mugler, Matthew C Tate, Marc W Slutsky, Dean J Krusienski, and Tanja Schultz. 2019. Speech synthesis from ecog using densely connected 3d convolutional neural networks. *Journal of neural engineering*, 16(3):036019.

Gopala K Anumanchipalli, Josh Chartier, and Edward F Chang. 2019. Speech synthesis from neural decoding of spoken sentences. *Nature*, 568(7753):493–498.

Sandesh Aryal and Ricardo Gutierrez-Osuna. 2016. Data driven articulatory synthesis with deep neural networks. *Computer Speech & Language*, 36:260–273.

Rohan Badlani, Adrian Łancucki, Kevin J Shih, Rafael Valle, Wei Ping, and Bryan Catanzaro. 2021. One tts alignment to rule them all. *arXiv preprint arXiv:2108.10447*.

Mathieu Bernard and Hadrien Titeux. 2021. **Phonemizer: Text to phones transcription for multiple languages in python**. *Journal of Open Source Software*, 6(68):3958.

Peter Birkholz. 2013a. Modeling consonant-vowel coarticulation for articulatory speech synthesis. *PloS one*, 8(4):e60603.

Peter Birkholz. 2013b. **Modeling consonant-vowel coarticulation for articulatory speech synthesis**. *PloS one*, 8:e60603.

Alan W Black. 2019. CMU wilderness multilingual speech dataset. In *ICASSP*, pages 5971–5975. IEEE.

619	Florent Bocquelet, Thomas Hueber, Laurent Girin, Pierre Badin, and Blaise Yvert. 2014. Robust articulatory speech synthesis using deep neural networks for bci applications. In <i>15th Annual Conference of the International Speech Communication Association (Interspeech 2014)</i> .	675
620		676
621		677
622		
623		
624		
625	Yu-Wen Chen, Kuo-Hsuan Hung, Shang-Yi Chuang, Jonathan Sherman, Wen-Chin Huang, Xugang Lu, and Yu Tsao. 2021. Ema2s: An end-to-end multi-modal articulatory-to-speech system. In <i>2021 IEEE International Symposium on Circuits and Systems (ISCAS)</i> , pages 1–5. IEEE.	678
626		679
627		680
628		681
629		682
630		683
631		684
632		
633		
634		
635	Tam'as G'abor Csap'o, Csaba Zaink'o, L. Viktor T'oth, Gábor Gosztolya, and Alexandra Mark'o. 2020. Ultrasound-based articulatory-to-acoustic mapping with wav2glow speech synthesis. In <i>Interspeech</i> .	685
636		686
637		687
638		688
639		689
640	Isaac Elias, Heiga Zen, Jonathan Shen, Yu Zhang, Jia Ye, R. J. Skerry-Ryan, and Yonghui Wu. 2021. Parallel tacotron 2: A non-autoregressive neural tts model with differentiable duration modeling. <i>ArXiv</i> , abs/2103.14574.	690
641		691
642		692
643		693
644		
645		
646	Gunnar Fant. 1991. What can basic research contribute to speech synthesis? <i>Journal of Phonetics</i> , 19(1):75–90.	694
647		695
648		696
649		697
650		698
651		
652		
653	Gunnar Fant. 1995. The lf-model revisited. transformations and frequency domain analysis. <i>Speech Trans. Lab. Q. Rep., Royal Inst. of Tech. Stockholm</i> , 2(3):40.	699
654		700
655		701
656		702
657		703
658	David Gaddy and Dan Klein. 2021. An improved model for voicing silent speech . In <i>Proceedings of the 59th Annual Meeting of the Association for Computational Linguistics and the 11th International Joint Conference on Natural Language Processing (Volume 2: Short Papers)</i> , pages 175–181, Online. Association for Computational Linguistics.	704
659		705
660		
661		
662		
663		
664		
665		
666	Marc-Antoine Georges, Pierre Badin, Julien Diard, Laurent Girin, Jean-Luc Schwartz, and Thomas Hueber. 2020. Towards an articulatory-driven neural vocoder for speech synthesis. In <i>International Seminar on Speech Production</i> .	706
667		707
668		708
669		709
670		710
671		711
672	Pengcheng Guo, Florian Boyer, Xuankai Chang, Tomoki Hayashi, Yosuke Higuchi, Hirofumi Inaguma, Naoyuki Kamo, Chenda Li, Daniel Garcia-Romero, Jiatong Shi, et al. 2021. Recent developments on espnet toolkit boosted by conformer. In <i>ICASSP 2021-2021 IEEE International Conference on Acoustics, Speech and Signal Processing (ICASSP)</i> , pages 5874–5878. IEEE.	712
673		713
674		714
675		715
676		716
677		
678	Awni Y. Hannun, Carl Case, Jared Casper, Bryan Catanzaro, Gregory Frederick Diamos, Erich Elsen, Ryan J. Prenger, Sanjeev Satheesh, Shubho Sengupta, Adam Coates, and A. Ng. 2014. Deep speech: Scaling up end-to-end speech recognition. <i>ArXiv</i> , abs/1412.5567.	717
679		718
680		719
681		720
682		721
683		
684		
685	Takamichi, and Shinji Watanabe. 2021. Espnet2-tts: Extending the edge of tts research. <i>arXiv preprint arXiv:2110.07840</i> .	722
686		723
687		724
688		725
689		726
690		727
691		
692		
693		
694	Hiroyuki Inaguma, Shun Kiyono, Kevin Duh, Shigeki Karita, Nelson Yalta, Tomoki Hayashi, and Shinji Watanabe. 2020. ESPnet-ST: All-in-one speech translation toolkit . In <i>Proceedings of the 58th Annual Meeting of the Association for Computational Linguistics: System Demonstrations</i> , pages 302–311, Online. Association for Computational Linguistics.	694
695		695
696		696
697		697
698		698
699	Khalil Iskarous, Louis Goldstein, Douglas H Whalen, Mark Tiede, and Philip Rubin. 2003. Casy: The haskins configurable articulatory synthesizer. In <i>International Congress of Phonetic Sciences, Barcelona, Spain</i> , pages 185–188.	699
700		700
701		701
702		702
703		703
704		704
705		705
706	Ye Jia, Ron Weiss, Fadi Biadsy, Wolfgang Macherey, Melvin Johnson, Zhifeng Chen, and Yonghui Wu. 2019. Direct speech-to-speech translation with a sequence-to-sequence model . In <i>Interspeech</i> , pages 1123–1127.	706
707		707
708		708
709		709
710		710
711		711
712	Ye Jia, Jungil Kong, and Juhee Son. 2021. Conditional variational autoencoder with adversarial learning for end-to-end text-to-speech . In <i>Proceedings of the 38th International Conference on Machine Learning</i> , volume 139 of <i>Proceedings of Machine Learning Research</i> , pages 5530–5540. PMLR.	712
713		713
714		714
715		715
716		716
717	Diederik P. Kingma and Jimmy Ba. 2015. Adam: A method for stochastic optimization . In <i>3rd International Conference on Learning Representations, ICLR 2015, San Diego, CA, USA, May 7-9, 2015, Conference Track Proceedings</i> .	717
718		718
719		719
720		720
721		721
722	Jungil Kong, Jaehyeon Kim, and Jaekyoung Bae. 2020. Hifi-gan: Generative adversarial networks for efficient and high fidelity speech synthesis . In <i>Advances in Neural Information Processing Systems</i> , volume 33, pages 17022–17033. Curran Associates, Inc.	722
723		723
724		724
725		725
726		726
727		727
728	Kevin Lenzo and Alan Black. 2000. Diphone collection and synthesis. <i>ICSLP</i> .	728
729		729

730	Yongwan Lim, Asterios Toutios, Yannick Bliesener, Ye Tian, Sajan Lingala, Colin Vaz, Tanner Sorensen, Miran Oh, Sarah Harper, Weiyi Chen, Yoonjeong Lee, Johannes Töger, Mairym Llorens Monteserín, Caitlin Smith, Bianca Godinez, Louis Goldstein, Dani Byrd, Krishna Nayak, and Shrikanth Narayanan. 2021. A multispeaker dataset of raw and reconstructed speech production real-time mri video and 3d volumetric images. <i>Scientific Data</i> , 8.	782
731		783
732		784
733		785
734		786
735		787
736		
737		
738		
739	Zheng-Chen Liu, Zhen-Hua Ling, and Li-Rong Dai. 2018. Articulatory-to-acoustic conversion using blstm-rnns with augmented input representation. <i>Speech Communication</i> , 99:161–172.	788
740		789
741		790
742		791
743	Max Morrison, Rithesh Kumar, Kundan Kumar, Prem Seetharaman, Aaron Courville, and Yoshua Bengio. 2022. Chunked autoregressive gan for conditional waveform synthesis. In <i>Submitted to ICLR 2022</i> .	792
744		793
745		794
746		795
747	Tomáš Nekvinda and Ondřej Dušek. 2020. One Model, Many Languages: Meta-Learning for Multilingual Text-to-Speech. In <i>Interspeech</i> , pages 2972–2976.	796
748		
749		
750	Vassil Panayotov, Guoguo Chen, Daniel Povey, and Sanjeev Khudanpur. 2015. Librispeech: an asr corpus based on public domain audio books. In <i>2015 IEEE international conference on acoustics, speech and signal processing (ICASSP)</i> , pages 5206–5210. IEEE.	802
751		803
752		804
753		805
754		806
755		807
756	Adam Polyak, Yossi Adi, Jade Copet, Eugene Kharitonov, Kushal Lakhotia, Wei-Ning Hsu, Abdellrahman Mohamed, and Emmanuel Dupoux. 2021. Speech Resynthesis from Discrete Disentangled Self-Supervised Representations. In <i>Interspeech</i> .	808
757		809
758		810
759		811
760		812
761	Ryan Prenger, Rafael Valle, and Bryan Catanzaro. 2019. Waveglow: A flow-based generative network for speech synthesis. In <i>ICASSP 2019 - 2019 IEEE International Conference on Acoustics, Speech and Signal Processing (ICASSP)</i> , pages 3617–3621.	813
762		
763		
764		
765		
766	Korin Richmond, Phil Hoole, and Simon King. 2011. Announcing the electromagnetic articulography (day 1) subset of the mngu0 articulatory corpus. In <i>Interspeech</i> , pages 1505–1508.	814
767		815
768		816
769		817
770	Philip Rubin, Thomas Baer, and Paul Mermelstein. 1981. An articulatory synthesizer for perceptual research. <i>The Journal of the Acoustical Society of America</i> , 70(2):321–328.	818
771		
772		
773		
774	Celia Scully. 1990. Articulatory synthesis. In <i>Speech production and speech modelling</i> , pages 151–186. Springer.	823
775		824
776		825
777	Berrak Sisman, Junichi Yamagishi, Simon King, and Haizhou Li. 2020. An overview of voice conversion and its challenges: From statistical modeling to deep learning. <i>IEEE/ACM Transactions on Audio, Speech, and Language Processing</i> .	826
778		827
779		
780		
781		
782	Simon Stone, Philipp Schmidt, and Peter Birkholz. 2020. Prediction of voicing and the f0 contour from electromagnetic articulography data for articulation-to-speech synthesis. In <i>ICASSP 2020-2020 IEEE International Conference on Acoustics, Speech and Signal Processing (ICASSP)</i> , pages 7329–7333. IEEE.	828
783		829
784		830
785		831
786		832
787		833
788	Fumiaki Taguchi and Tokihiko Kaburagi. 2018. Articulatory-to-speech conversion using bi-directional long short-term memory. In <i>Interspeech</i> , pages 2499–2503.	834
789		
790		
791		
792	Andros Tjandra, Sakriani Sakti, and Satoshi Nakamura. 2019. Speech-to-speech translation between untranscribed unknown languages. In <i>2019 IEEE Automatic Speech Recognition and Understanding Workshop (ASRU)</i> , pages 593–600.	835
793		836
794		837
795		838
796		
797	Ashish Vaswani, Noam Shazeer, Niki Parmar, Jakob Uszkoreit, Llion Jones, Aidan N Gomez, Łukasz Kaiser, and Illia Polosukhin. 2017. Attention is all you need. In <i>Advances in Neural Information Processing Systems</i> , volume 30. Curran Associates, Inc.	839
798		840
799		841
800		842
801		
802	Xin Wang, Shinji Takaki, and Junichi Yamagishi. 2019. Neural source-filter-based waveform model for statistical parametric speech synthesis. In <i>ICASSP 2019 - 2019 IEEE International Conference on Acoustics, Speech and Signal Processing (ICASSP)</i> , pages 5916–5920.	843
803		844
804		845
805		846
806		847
807		
808	Yuxuan Wang, R. J. Skerry-Ryan, Daisy Stanton, Yonghui Wu, Ron J. Weiss, Navdeep Jaitly, Zongheng Yang, Ying Xiao, Z. Chen, Samy Bengio, Quoc V. Le, Yannis Agiomyrgiannakis, Robert A. J. Clark, and Rif A. Saurous. 2017. Tacotron: Towards end-to-end speech synthesis. In <i>Interspeech</i> .	848
809		849
810		850
811		851
812		852
813		
814	Peter Wu, Paul Pu Liang, Jiatong Shi, Ruslan Salakhutdinov, Shinji Watanabe, and Louis-Philippe Morency. 2021a. Understanding the tradeoffs in client-side privacy for downstream speech tasks. In <i>APSIPA ASC</i> .	853
815		854
816		855
817		856
818		
819	Peter Wu, Jiatong Shi, Yifan Zhong, Shinji Watanabe, and Alan W Black. 2021b. Cross-lingual transfer for speech processing using acoustic language similarity. In <i>ASRU</i> .	857
820		858
821		859
822		
823	Chengzhu Yu, Heng Lu, Na Hu, Meng Yu, Chao Weng, Kun Xu, Peng Liu, Deyi Tuo, Shiyin Kang, Guangzhi Lei, et al. 2019. Durian: Duration informed attention network for multimodal synthesis. <i>arXiv preprint arXiv:1909.01700</i> .	860
824		861
825		862
826		863
827		
828	Yu Zhang, Ron J Weiss, Heiga Zen, Yonghui Wu, Zhipeng Chen, RJ Skerry-Ryan, Ye Jia, Andrew Rosenberg, and Bhuvana Ramabhadran. 2019. Learning to speak fluently in a foreign language: Multilingual speech synthesis and cross-language voice cloning. <i>arXiv preprint arXiv:1907.04448</i> .	864
829		865
830		866
831		867
832		868
833		
834	A Appendix	869

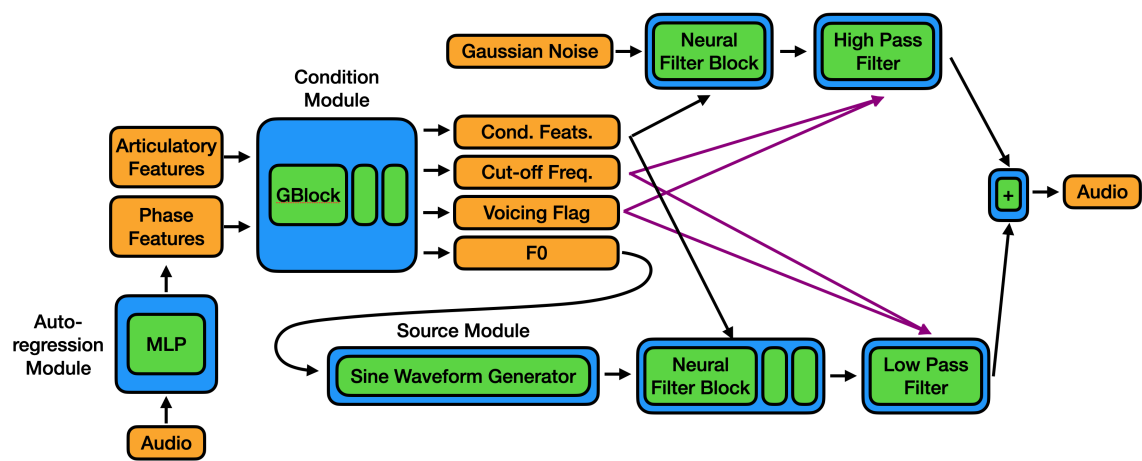


Figure 7: Model architecture of our NSF-CAR generator.